IEEE Access
Multidisciplinary | Rapid Review | Open Access Journal

Received January 29, 2018, accepted February 26, 2018, date of publication March 9, 2018, date of current version April 18, 2018.

Digital Object Identifier 10.1109/ACCESS.2018.2813319

Rail Profile Measurement Based on Line-structured Light Vision

PENG ZHOU[1], KE XU[2], AND DADONG WANG[3]

[1]Institute of Engineering Technology, University of Science and Technology Beijing, Beijing 100083, China
[2]Collaborative Innovation Center of Steel Technology, University of Science and Technology Beijing, Beijing 100083, China
[3]Quantitative Imaging Research Team, Data61, CSIRO, Sydney, NSW 2122, Australia

Corresponding author: Peng Zhou (zhoupeng@nercar.ustb.edu.cn)

This work was supported in part by the National Natural Science Foundation of China under Grant 51674031 and in part by the Fundamental Research Funds for the Central Universities under Grant FRF-TP-16-018A1.

ABSTRACT High-speed railway in China has undergone rapid development in recent years. Technology for structure measurement is recognized as an important aspect of steel rail quality inspection. The shape of the rail welding base is mainly gauged using mechanical contact measurement technology. Matching this technology with the escalating demands for quality inspection of steel rails is a challenging task. In this paper, a structured light measurement approach is proposed and employed which intersects the rail through the structural light plane projected by inner and outer laser sensors. These sensors form a laser light stripe curve containing the profile information of the rail surface. By processing laser light bars using image analysis and contour reduction techniques, 3-D profiles of the rails are generated. The laser plane is fitted using the coordinate points of the laser light bars converted between the image and world coordinate systems. A new calibration method based on the parallel moving target for line-structured light is proposed to improve the calibration and address the issue caused by the limited number of the extracted calibration points during free target calibration. The rail profile, including the geometric dimension, straightness, and twist of the rail, are then measured. By comparing the measured profile with the standard contour of the rails, the rail wear can then be quantitatively assessed. The experimental results show that the proposed measurement system outperforms the traditional single index detection.

INDEX TERMS Three-dimensional (3D) reconstruction, structured light, measurement, machine vision.

I. INTRODUCTION

The rapid development of high-speed railway in China has greatly promoted the economic growth of the country and also resulted in greater demands for high-quality rails.

Rails are currently produced by rolling the rail in advance according to specified roller parameters. The product quality is then inspected. The roller parameters are adjusted according to the rail sizes. These alterations can cause the manufacture of numerous products which do not meet specifications. This leads to increased production costs and energy consumption along with financial loss to enterprises. An online profile measuring device that provides accurate rail profile information to feed the rolling mill in real-time is required to monitor the product quality and avoid the continuous production of unqualified products. In addition, the geometrical size, straightness and distortion of the rail section also has significant influence on the safety and smooth operation of a train [1].

Three-dimensional (3D) data acquisition techniques for measuring the rail profile include contact and non-contact approaches. Contact measurement is also called mechanical measurement, and a 3D coordinate measuring machine is primarily used in this approach. In this technique, a probe contact is used to scan the entire surface of the rail to acquire the 3D contour data. Although the technology has been applied in many fields, its inherent shortcomings have become more evident because of rapid developments in science and technology, its slow measurement, and the need for equipment maintenance.

Non-contact measurement has emerged with the rapid development of machine learning algorithms in human-centered systems [2]–[5], optics and computer measurement technologies, and breakthroughs in the performance of charge-coupled devices (CCD) and projectors. This approach includes various optical 3D measurement technologies with the following advantages: contact between objects is not

required during measurement; rapid measurement and calculation; and high measurement accuracy. Hence, the non-contact optical 3D measurement technology has been widely applied in industrial production.

There are two types of non-contact optical 3D measurement technologies, namely passive and active, based on their imaging illumination. Passive 3D measurement is represented by binocular vision technology and the focal gradient method. This approach uses an unstructured lighting mode. Binocular vision technology originates from bionics. Similar systems of human binocular vision are built by simulation, and the distance information extracted from two different vision directions of two-dimensional images. Early developments of this technology were difficult to apply because of slow computation on large amounts of data and extreme dependence on the texture features of the object being measured. Recently, with improvements in computer hardware performance the technology has seen gradual uptake in application to human systems [6], [7]. Passive 3D focal gradient has slowly developed and infrequently used in practice since it was first proposed [8]. The technology first obtains two defocused images of the measured object and then calculates the relative ambiguity of these images, which is a key parameter. Finally, the 3D structure of the object is solved according to the relation between the relative fuzzy degree and fuzzy parameters of the optical system.

Passive 3D measurement technology is not suitable for precise metrology because of its limitations such as low accuracy, large computation and so on. It is usually used for 3D object recognition and configuration analysis. However, the structure of this technology is simple, data acquisition is convenient, and it has been used in machine vision applications.

Active 3D measurement has been used in computer vision since it was originally proposed in 1971 [9]. This technology uses active structural light technology and is the most considered 3D measurement technology by researchers. According to its theoretical model, a pair of optical signal launchers and receiving devices can be placed to complete data acquisition. The image information of structured light modulated by the 3D surface of an object is obtained by an optical signal receiving device. Variable structured light is projected according to a certain rule to the surface of the object being measured. Finally, the 3D surface data of the object surface can be obtained quickly after computation. Ative 3D measurement technology is highly precise, rapid, and robust. Thus, this technology has been widely applied in various applications and can be classified into the following categories:

A. TIME OF FLIGHT (TOF)

The principle of the 3D measurement using TOF is not complicated. The pulse signal is continuously transmitted to the object surface through laser, and then the pulse signal from the object surface is received by the sensor. Finally, the target distance is obtained by measuring the flying time of the laser pulse. The system is simple in structure, with only one laser and a signal receiver. There are two conditions for this type of application. First, the pulse launcher and the signal receiving device should always be synchronized. Second, the TOF must be provided by the receiving device. This method requires high time resolution of the signal processing system to achieve high measurement accuracy, and has been applied in various applications. One application particularly well suited for TOF is real-time depth keying in dynamic 3D scenes [10], where the TOF technique facilitates true 3D segmentation and 3D object insertion [11], [12].

B. MOIRÉ PROFILOMETRY (MP)

MP, which was first proposed in 1970 [13], involves 3D contour measurement using Moiré fringes. A reference grating is projected on the surface of a 3D object, and the grating stripe is deformed because of the change in the height of the object surface. Thus, a deformed grating is obtained. Then, the Moiré fringes are obtained by superimposition of the datum grating and the deformed grating. The Moiré fringe contains information of the surface of the measured object.

C. FRINGE PROJECTION PROFILOMETRY (FPP)

FPP for 3D surface measurement is a multistep technique. A structured light image with continuous phase change (usually a sinusoidal image) is projected to the surface of the object and the reference plane in turn using a digital projector. Then, a CCD camera is used to record the stripe images modulated from the surface of the object and the stripe images on the reference plane. Phase information is obtained by analyzing the striped images collected. A phase unwrapping algorithm is then used to obtain continuous phase distribution corresponding to the object surface. Finally, the system is calibrated to transform the information of the continuous phase distribution into the true height information of the object surface. FPP has been widely used in 3D model acquisition [14] and magnetic resonance imaging [15]. However, this method is limited by stripe distortion, difficult selection and placement of reference plane plates, and mirror reflection on the surface of the rail.

D. LASER TRIANGULATION (LT)

LT is also called structural light measurement and is based on laser projection profile measurement. First, the beam from the laser source is projected on the outer surface of the object being measured, and then the reflected light is received by the signal receiver. When the surface height changes, the image formed in the detector also has relative displacement. The 3D shape of the object can be measured according to the relationship between the change in actual height and the change of the imaging displacement. The technique is robust to changes in ambient light [16] and has been applied to rail profile measurements. In [17], the structured light technique is used to extract the condition of rails (through rail profile measurements) and detect surface defects. The structural light method has been used to extract rail profiles from real images [18], [19]. The images are processed

by recognizing the rail track, extracting the laser stripe center [20], and calibrating cameras [21].

Given that structural light 3D vision has wide range and large field of view, highly accurate video field, high precision, and its light strip image information can be simply extracted on a real-time basis [22], this technology is increasingly applied in industrial inspection and measurement. In this article, we present an improved method based on this technology and have successfully applied it to the detection and measurement of a rail cross section. The main contribution of this paper include:

(1) The rail cross section is measured in all directions with the combination of multiple cameras and lasers. The profile of the rail section is obtained by coordinate transformation. The camera is controlled with a certain time interval to capture the images of the rail driven by a mobile console to carry out one-dimensional scan, and 3D reconstruction of the rail is realized. After obtaining the rail profile, the distance from point to line is used as the straightness of rail and the distance from point to plane used as the twist degree of rail. Thus, the measurement of rail size, straightness, and twist degree is obtained.

(2) A customized image analysis routine is used to process the image of the laser line. A morphological thinning method is used to calculate the coordinates of laser lines in the image coordinate system. This not only reduces the computation but also obtains the exact coordinates.

(3) Calibration of the free target is improved, and the method of structured light for the parallel moving target is proposed and implemented. This method does not need to extract the mark points but converts all coordinates of the light bars to the world coordinate system. Meanwhile, the calibration error is reduced by fitting the light plane equation.

II. MATHEMATICAL MODELING

In this section we analyze the measurement system and structured light methods.

A. CAMERA SENSOR MEASUREMENT MODEL

During camera calibration, several coordinate systems are established. These systems include image pixel coordinate system o-uv (unit: pixel), image physical coordinate system O-xy (unit: millimeter), camera coordinate system $O_c - X_cY_cZ_c$ (unit: millimeter), and the world coordinate system $O_{wi} - X_{wi}Y_{wi}Z_{wi}$ (unit: millimeter).

The projection relation between the 3D object space and the imaging plane is the imaging model, and for the camera, there is a small aperture imaging model, an orthogonal projection model, and a quasi-perspective projection model. The small aperture imaging model is simple and practical without losing accuracy, and lens distortion is not considered. The advantage of this model is the linear imaging relation. That is, the light reflected on the object surface is projected onto the image plane through a pinhole. This characteristic satisfies the straight line propagation of light. The following equation (1) represents a camera perspective projection model.

$$s\begin{bmatrix} u \\ v \\ 1 \end{bmatrix} = \begin{bmatrix} f_x & 0 & u_0 & 0 \\ 0 & f_y & v_0 & 0 \\ 0 & 0 & 1 & 0 \end{bmatrix} \begin{bmatrix} R & T \\ 0 & 1 \end{bmatrix} \begin{bmatrix} X_w \\ Y_w \\ Z_w \\ 1 \end{bmatrix} = \begin{bmatrix} m_{11} & m_{12} & m_{13} & m_{14} \\ m_{21} & m_{22} & m_{23} & m_{24} \\ m_{31} & m_{32} & m_{33} & m_{34} \end{bmatrix} \begin{bmatrix} X_w \\ Y_w \\ Z_w \\ 1 \end{bmatrix} \quad (1)$$

where s is a nonzero scale factor; u and v are the coordinates of the image pixel coordinates; f_x and f_y are the projection of the effective focal length in the X- and Y- axes, respectively, in pixels; and u_o and v_o are the main center coordinates, which are the image intersection coordinates between the image plane and optical axis. The 3×3 rotation matrix R and 3×1 translation vector t are the external parameters of the camera. (X_w, Y_w, Z_w) is the coordinate of a point in the world coordinate system.

First, the image pixel coordinates u and v are calculated by processing the image collected by the camera. Next, the internal and external parameters of the camera can be obtained by calibrating the camera. Then, the structured light method is used to obtain the structural light plane equation. Finally, the combination of the above can be used to find any point coordinate (X_w, Y_w, Z_w) in the world coordinate system.

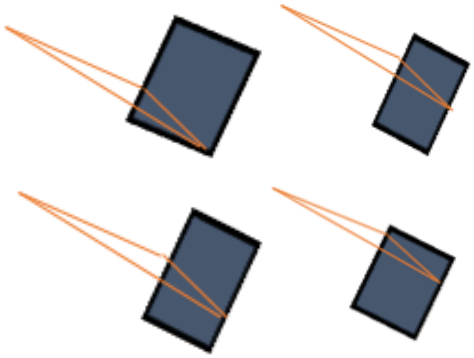

FIGURE 1. Laser line images on calibration boards with different positions.

B. STRUCTURED LIGHT METHOD WITH PARALLEL MOVING TARGET TO SOLVE PARAMETERS

When the laser illuminator is added to the system, a coordinate system or equation is needed to describe the location of the light source [23]. In this article, the coordinates of the 3D world point are solved by increasing the equation of the laser plane. The calibration board is moved in parallel, and laser line images on calibration boards with different positions are collected (Fig. 1). The X- and Y- axes of each moving target are used as the local world coordinate system to calculate the relative position between the camera coordinate system and the local world coordinate system R_i and t_i. Then, the first local world coordinate system is selected as the absolute

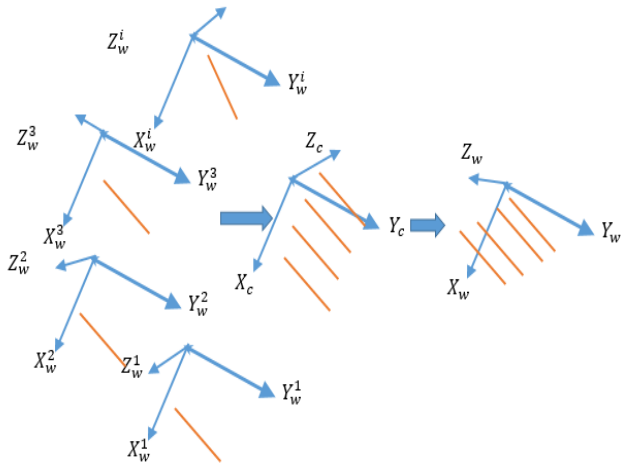

FIGURE 2. Coordinate transformation

world coordinate system from the N local world coordinate systems established above. Using the camera coordinate system as a bridge, the other $N-1$ local world coordinates are converted to the camera coordinate system using the external parameter matrix. Then, the camera coordinate system is transformed to the absolute world coordinate system (Fig. 2). Light plane $Z = AX + BY + C$ is fitted in the absolute world coordinate system (Fig. 3). The relative position of the light plane and the camera is then determined.

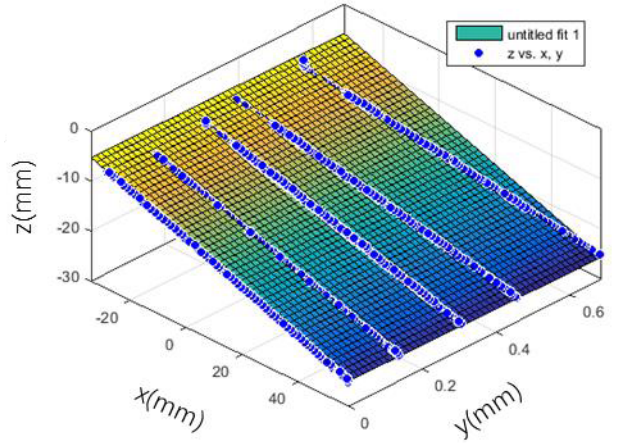

FIGURE 3. Light plane fitting.

The fitting light plane equation is brought into the camera perspective projection model, and equation (2) is then obtained. We can solve the 3D coordinate point of an object based on the calibrated parameters and the equation of the light plane.

$$\begin{cases} (u_i m_{31} + m_{11})X_w + (u_i m_{32} - m_{12})Y_w \\ \quad +(u_i m_{33} - m_{13})Z_w = m_{14} - u_i m_{34} \\ (v_i m_{31} + m_{21})X_w + (v_i m_{32} - m_{22})Y_w \\ \quad +(v_i m_{33} - m_{23})Z_w = m_{24} - v_i m_{34} \\ AX + BY + C = Z \end{cases} \tag{2}$$

The rail profile point (X_w, Y_w, Z_w) in the world coordinate system can be obtained by Equation (2), and then a one-dimensional scan is used to reconstruct the rail profile.

The comparison is conducted among the parallel moving target structured light method and other line structured light vision calibration methods based on the free moving plane target [24]. The traditional free moving plane target calibration is based on the extraction of the coordinates of the calibration points from both the phase plane coordinate system and the world coordinate system. Thus, the number of calibration points in the computer image coordinate and the world coordinate system can be used to solve the unknown parameters R and t of the line structured light vision sensor. There are two issues associated with this method. First, the extraction of the coordinates in the phase plane results in significant errors. When the laser plane is projected onto the plane target, a bright stripe is formed, and the intersection point between the light bar and the target black block is considered as the reference point. The intersection between the laser line and the chessboard is difficult to extract because of the difficulties in selecting the threshold and accurate positioning. Second, the number of calibrated points is limited, resulting in a large error in the presence of a calibrated point error. Therefore, gross error is difficult to avoid. With the method proposed in this article, there is no need to extract the standard point, all coordinates of the light bar are converted into the world coordinate system. The equation of the light plane is then fitted to reduce the error.

III. DATA PROCESSING AND MEASUREMENT PRINCIPLE

A. IMAGE PROCESSING

Image processing is performed to extract the laser stripe and refine its width into 1 pixel. This process includes denoising, histogram equalization, extracting regions of interest, binarization, and image thinning. The original image of the laser line taken by a camera is shown in Fig. 4(a). OTSU method is used to obtain a binary image [Fig. 4(b)], and then the binary image is thinned, and the skeleton of the binary image shown in Fig. 4(c) is obtained. Many burrs could appear after the thinning. Thus, the image deburring method is used to obtain the smooth image shown in Fig. 4(d).

B. SIZE CALCULATION

When the 3D contour is obtained, the dimension of the section can be calculated according to the coordinate point. The size calculation method is described as follows:

1) Rail height = Y coordinate of the highest point – Y coordinate of the lowest point;

2) Rail head width = | the X coordinate of the point 16 m lower than the highest point on the right – the X coordinate of the point 16 m lower than the highest point on the left |;

3) Rail base width = | the X coordinate of the point with maximum X coordinate – X coordinate value of the point with minimum X coordinate |;

4) Right rail foot height = |Y coordinate of the corresponding point after the point with maximum X coordinate moves 4 mm to the left – Y coordinate of the lowest point |;

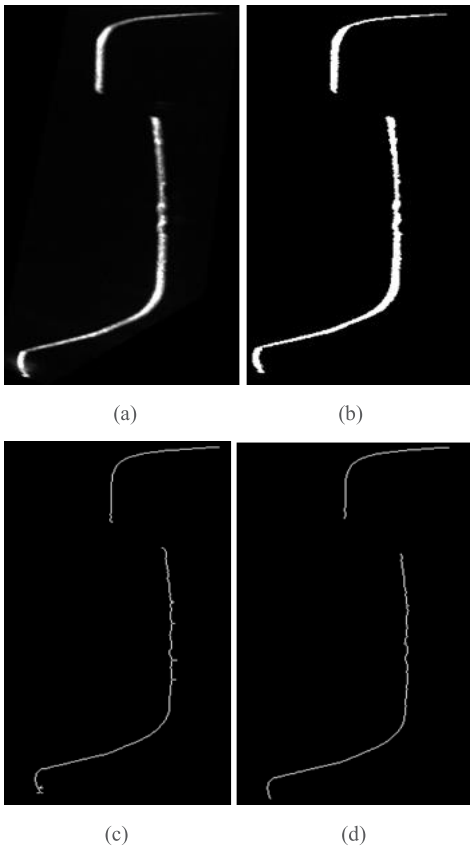

FIGURE 4. Image processing of the laser line. (a) Laser line image. (b) Binarization. (c) Thinning. (d) Burrs removal.

5) Rail waist thickness = | the difference between two X coordinates of the two corresponding points in the horizontal direction after the lowest point moves upwards 79 mm |;

6) Asymmetry = |X coordinate of the point with minimum X coordinate value – the X coordinate of the point 16 m lower than the highest point |.

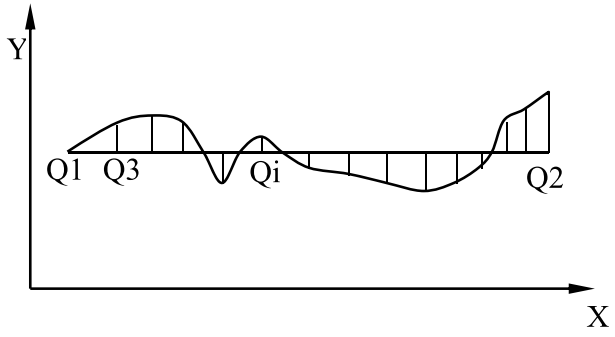

FIGURE 5. Measurement principle of straightness

C. MEASUREMENT OF STRAIGHTNESS AND DISTORTION

Straightness is calculated as shown in Fig. 5. The curve $Q1Q2$ is the longitudinal surface profile of the rail. The first and the last measurement points are connected in a straight line as a benchmark. Straightness is the max distance from the other middle point to the straight line, that is, max ($Q3$, $Q4$, ... Q_i).

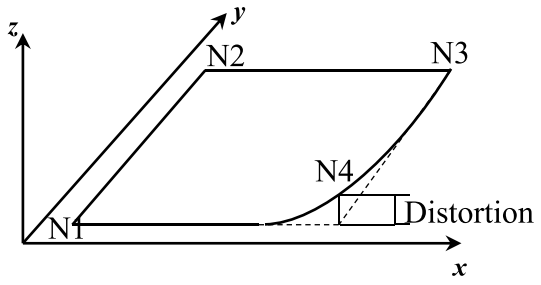

FIGURE 6. Measurement principle of distortion.

The distortion of the rail refers to the longitudinal distortion of the rail [25]. Two distortion calculation points N1 and N2 are considered at the top of the rail, and another two distortion calculation points N3–N4 are considered at the top surface of the cross section at the spot which is 1 meter from the rail end (Fig. 6). The distortion of the rail is calculated using the distance from the point to the plane. This process is performed by first finding the plane where N1–N2–N3 is located. The degree of distortion is the distance from N4 to the plane.

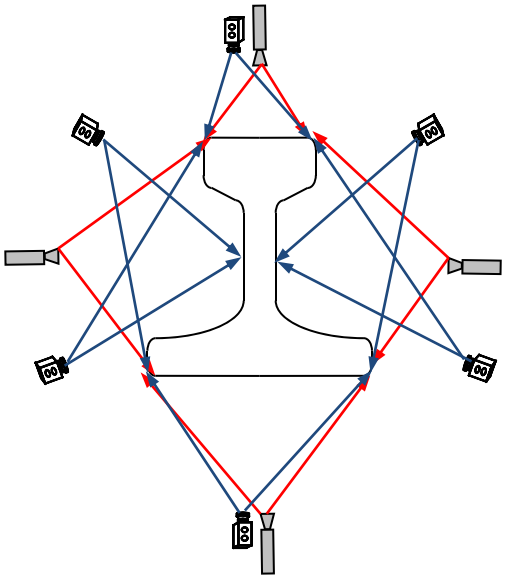

FIGURE 7. A schematic diagram of the designed system for measuring rail profile.

IV. EXPERIMENTAL RESULTS

A. MEASUREMENT SYSTEM DESIGN

In the measurement system, four groups of laser camera sensors are used. As shown in Fig. 7, a camera and a line-structured light source are used at both the top and bottom surfaces. Each side is composed of two cameras and a

FIGURE 8. The measured steel rail.

TABLE 1. In-camera parameters.

CCD	F_X	F_Y	U_0	V_0	K_1	K_2
1	1598.4	1530.6	379.83	262.33	0.4880	-24.5571
2	1534.7	1567.9	389.53	592.73	-0.3984	0.7986

line-structured light source. The laser is installed at different positions on each surface and is vertically irradiated with the surface of the rail. The side camera is used to acquire images at 45° with the normal line [26], and the interior and exterior laser camera sensors intersect the structural plane of light with the rail, forming a laser strip curve embedding the profile information of the rail surface. The camera and the structured light plane take a certain angle to shoot the rail laser contour image. The rail profile detection is realized based on laser triangulation.

The electric station controller controls the rotation of the motor and then the translation of the guide rail to drive the rail to shift to realize one-dimensional scanning. During this period, the camera collects rail images at the frame rate of 300fps and they can be used to generate the contours of the rail in different positions. The collected data are combined to reconstruct the rail profile. Fig. 8 shows the measured rail profile.

B. STRUCTURAL LIGHT CALIBRATION

After calibrating through a checkerboard board, the internal parameters of the left and right cameras are obtained (Table 1).

For the laser light plane fitting, The concrete realization process is as follows: 1) Break off the laser power, and shoot a chessboard target image. Then, extract the corner points and obtain their image coordinates. We set up the local world coordinate system on the target. After plug the corner into equation (1), we get the relationship between the local coordinate system and the camera coordinate system[R1 t1]. 2) Keep the target position of the chessboard unchanged and open the laser power. We use cameras to take the laser line and thin the image with morphology. 3) Moving the chessboard target forward and repeating the first two steps, we can get the laser stripes produced by the intersecting of laser plane and target and the [Ri ti]. 4) There we repeat the above operation 5 times, and select the target of first position as the absolute world coordinate system. Then the location of each straight line is converted into the camera coordinate system by [Ri ti]. 5) Finally, all points are converted to the absolute world coordinate system, we get 5 lines in the world coordinate system. By using the 5 sets of line point data, we obtained the fitted light plane equation $Z = -0.2149X - 0.9270Y - 12.5080$. Finally, the plane equation is combined with the camera model to determine the contour points in the world coordinate system.

C. 3D RECONSTRUCTION

The outline of the left and right sides should be joined to obtain a complete rail profile. Stitching is performed by choosing the same world coordinate system on both sides. Two stitched images are shown in Fig. 9. The resulting image is the outline of a certain position of the rail. and can only reflect the rail section at that position. The one-dimensional rail should be scanned to reconstruct the rail shape to obtain the overall rail profile. The reconstruction results are shown in Fig. 10.

For the spliced contour, the dimension is measured according to the algorithm of size calculation. Table 2 shows the measurement results for the length of 10 sections of a rail being tested.

Table 2 shows that the mean error of the measured parameters of the rail is in the range of 0.01 – 0.3 mm. Fig. 11 lists the straightness at each position of the rail. The distortion of

TABLE 2. Geometrical dimensions of rail sections.

SEQUENCE NUMBER	RAIL HEIGHT (H) MM	RAIL HEAD WIDTH MM	RAIL BASE WIDTH MM	RAIL WAIST THICKNESS MM	ASYMMETRY MM	RIGHT RAIL FOOT HEIGHT MM
1	176.53	70.40	149.13	16.33	40.94	10.25
2	176.33	70.39	149.17	16.84	40.94	10.25
3	176.45	70.39	149.10	17.88	40.92	10.25
4	175.66	70.39	149.35	16.29	40.91	13.10
5	176.64	70.14	149.21	17.37	41.37	9.64
6	176.69	69.89	149.23	16.29	40.94	10.25
7	176.95	70.68	149.20	15.78	40.44	10.94
8	175.62	70.75	149.59	16.80	41.03	13.12
9	175.67	70.75	149.53	16.81	41.00	13.11
10	176.63	70.93	149.89	16.29	40.85	9.11
MEAN	176.23	71.03	149.98	17.02	40.98	11.29
STANDARD VALUE	176 ± 0.6	70.8 ± 0.5	150	$16.5^{+1.0}_{-0.5}$	39.6 ± 1.2	12 ± 0.5
MEAN OF ERROR	0.23	0.23	-0.01	0.3.	0.12	-0.10

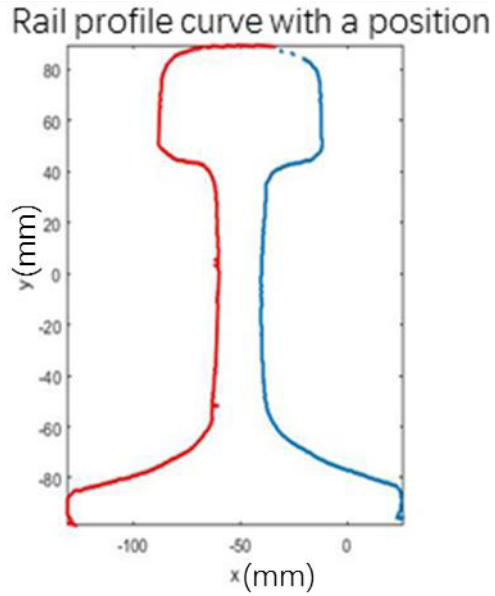

FIGURE 9. Section profile of the steel rail.

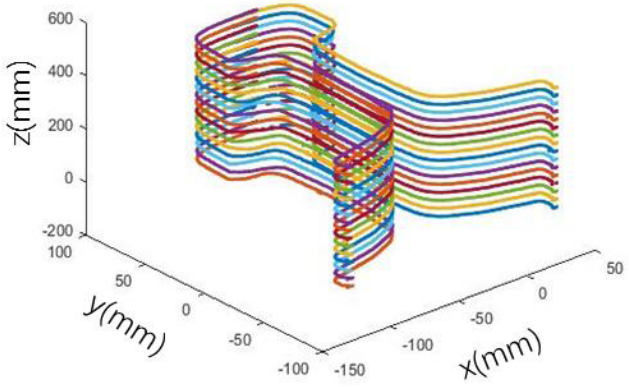

FIGURE 10. Contours of the rails spliced together.

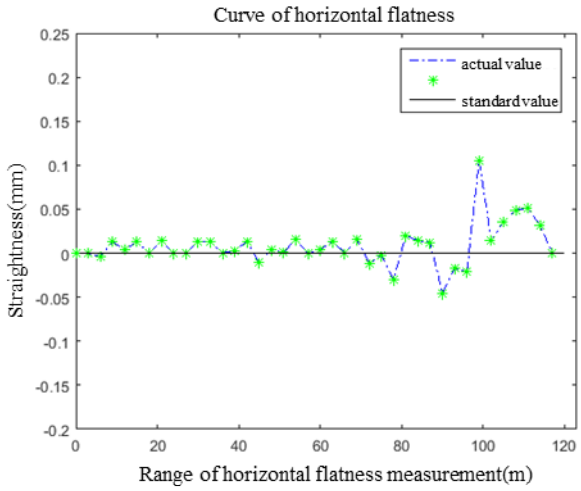

FIGURE 11. Curve of horizontal flatness.

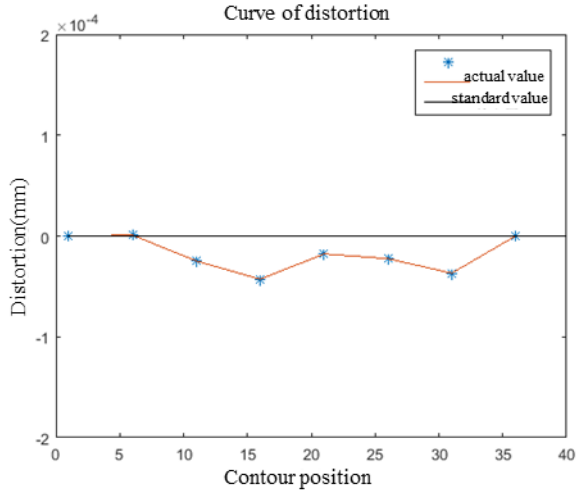

FIGURE 12. The Curve showing the rail distortion measurement.

the rail is reflected by the twist degree, shown as a curve of the distortion values in Fig. 12.

The profile of the rail is inspected by measuring its geometric dimension, straightness, and twist. By comparing the profile with the standard contour of the rail, the rail wear can be quantitatively measured. Thus, the proposed measurement method has many advantages over the present single index detection system.

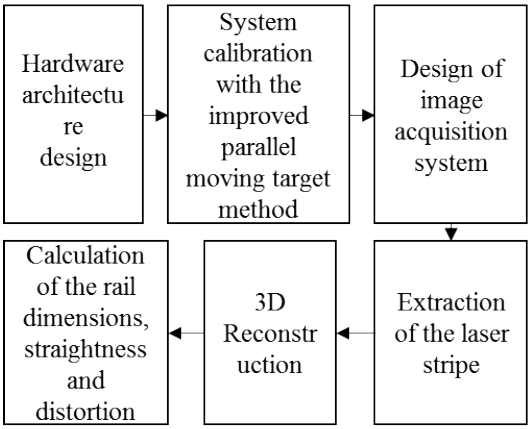

FIGURE 13. Architecture of the presented system.

V. CONCLUSION

In this article, we present an improved structured light measurement system (as shown in Fig. 13) which can be used to dynamically measure the profile of a rail. The system proposed is based on a parallel moving target structured light method, an improved calibration method of free target, and the reconstructed 3D contour of the rail. Detailed hardware and measurement algorithms are reported, including laser image analysis routines, accurate extraction of center line of the laser image of a rail, conversion of different coordinate systems and calculation of the rail dimensions and profile. Experimental results show that the proposed system has high measurement accuracy and is practically useful for both rail profile and wear measurement.

The proposed method can be potentially used in other industrial applications. In the future, we will explore opportunities to employ machine learning to further improve the models used in the measurement system.

REFERENCES

[1] D. S. Chen and Q. R. Xu, *GJ-5 Road Inspection Car*. Beijing, China: China Railway Publishing House, 2013.
[2] W. Zhao *et al.*, "A human-centered activity tracking system: Toward a healthier workplace," *IEEE Trans. Human–Mach. Syst.*, vol. 47, no. 3, pp. 343–355, Jun. 2017.
[3] X. Luo *et al.*, "Towards enhancing stacked extreme learning machine with sparse autoencoder by correntropy," *J. Franklin Inst.*, vol. 355, no. 4, pp. 1945–1966, Mar. 2018, doi: 10.1016/j.jfranklin.2017.08.014.
[4] M. Huang, A. Liu, T. Wang, and C. Huang, "Green data gathering under delay differentiated services constraint for Internet of Things," *Wireless Commun. Mobile Comput.*, vol. 2018, Feb. 2018, Art. no. 9715428. [Online]. Available: http://downloads.hindawi.com/journals/wcmc/aip/9715428.pdf, doi: 10.1155/2018/9715428.
[5] X. Luo, J. Deng, J. Liu, W. Wang, X. Ban, and J.-H. Wang, "A quantized kernel least mean square scheme with entropy-guided learning for intelligent data analysis," *China Commun.*, vol. 14, no. 7, pp. 1–10, Jul. 2017.
[6] A. Baumberg, A. Lyons, and R. Taylor, "3D S.O.M.—A commercial software solution to 3D scanning," *Graph. Models*, vol. 67, no. 6, pp. 476–495, Nov. 2003.
[7] C. Ttofis, C. Kyrkou, and T. Theocharides, "A low-cost real-time embedded stereo vision system for accurate disparity estimation based on guided image filtering," *IEEE Trans. Comput.*, vol. 65, no. 9, pp. 2678–2693, Sep. 2016.
[8] A. P. Pentland, "A new sense for depth of field," *IEEE Trans. Pattern Anal. Mach. Intell.*, vol. PAMI-9, no. 4, pp. 523–531, Jul. 1987.
[9] N. Chiba, S. Arai, and K. Hashimoto, "Feedback projection for 3D measurements under complex lighting conditions," in *Proc. Amer. Control Conf.*, Seattle, WA, USA, May 2017, pp. 4649–4656.
[10] A. Kolb, E. Barth, and R. Koch, "ToF-sensors: New dimensions for realism and interactivity," in *Proc. IEEE CVPR*, Anchorage, AK, USA, Jun. 2008, pp. 1–6.
[11] G. J. Iddan and G. Yahav, "Three-dimensional imaging in the studio and elsewhere," *Proc. SPIE*, vol. 4298, pp. 48–55, Apr. 2001.
[12] G. A. Thomas, "Mixed reality techniques for TV and their application for on-set and pre-visualization in film production," in *Proc. Int. Workshop Mixed Reality Technol. Filmmaking*, 2006, pp. 31–36.
[13] D. T. Moore and B. E. Truax, "Phase-locked Moiré fringe analysis for automated contouring of diffuse surfaces," *Appl. Opt.*, vol. 18, no. 1, pp. 91–96, 1979.
[14] B. Budianto, P. K. D. Lun, and T.-C. Hsung, "Marker encoded fringe projection profilometry for efficient 3D model acquisition," *Appl. Opt.*, vol. 53, no. 31, pp. 7442–7453, 2014.
[15] M. Arevalillo-Herráez, M. Cobos, and M. García-Pineda, "A robust wrap reduction algorithm for fringe projection profilometry and applications in magnetic resonance imaging," *IEEE Trans. Image Process.*, vol. 26, no. 3, pp. 1452–1465, Mar. 2017.
[16] J. Salvi, S. Fernandez, T. Pribanic, and X. Llado, "A state of the art in structured light patterns for surface profilometry," *Pattern Recognit.*, vol. 43, no. 8, pp. 2666–2680, Aug. 2010.
[17] V. Rikhotso, N. Steyn, and Y. Hamam, "3D rail modelling and measurement for rail profile condition assessment," in *Proc. IEEE AFRICON*, Cape Town, South Africa, Sep. 2017, pp. 1522–1527.
[18] C. Alippi, E. Casagrande, F. Scotti, and V. Piuri, "Composite real-time image processing for railways track profile measurement," *IEEE Trans. Instrum. Meas.*, vol. 49, no. 3, pp. 559–564, Jun. 2000.
[19] Z. Liu, J. H. Sun, H. Wang, and G. J. Zhang, "Simple and fast rail wear measurement method based on structured light," *Opt. Lasers Eng.*, vol. 49, no. 11, pp. 1343–1351, Nov. 2011.
[20] J.-H. Sun, H. Wang, Z. Liu, and G. J. Zhang, "Rapid extraction algorithm of laser stripe center in rail wear dynamic measurement," *Opt. Precis. Eng.*, vol. 19, no. 6, pp. 690–696, 2011.
[21] Z. Zhang, "A flexible new technique for camera calibration," *IEEE Trans. Pattern Anal. Mach. Intell.*, vol. 22, no. 11, pp. 1330–1334, Nov. 2000.
[22] G. J. Zhang and T. Xu, "Structured light 3-D vision and its industry application," (in Chinese), *J. Beijing Univ. Aeron. Astron.*, vol. 22, no. 6, pp. 650–654, 1996.
[23] G. Q. Sun, Z. P. Xu, and Y. Q. Wang, "A global calibration method for line structured-light 3D measure system," (in Chinese), in *Proc. 13th Nat. Conf. Image Graph.*, 2006, pp. 6–10.
[24] J. H. Sun, G. J. Zhang, and Q. Z. Liu, "Universal method for calibrating structured-light vision sensor on the spot," (in Chinese), *J. Mech. Eng.*, vol. 45, no. 3, pp. 174–177, 2009.
[25] W. Li, L. Li, Z. K. Gao, and W. Ding, "Digital rail contour detection," (in Chinese), *Railway Eng.*, vol. 6, no. 9, pp. 125–127, Sep. 2014.
[26] P. Zhou and K. Xu, "On-linesurface defect detection for steel rails based on multi-line lasers," (in Chinese), *J. Eng. Sci.*, vol. 37, no. 1, pp. 18–23, 2015.

PENG ZHOU received the Ph.D. degree from the University of Science and Technology Beijing, China, in 2015. He is currently an Assistant Researcher with the Institute of Engineering Technology, University of Science and Technology Beijing. His research interests include image processing, signal processing, and machine vision.

KE XU is currently a Full Professor with the Institute of Engineering Technology, University of Science and Technology Beijing, China. His research interests include image processing and surface quality detection technology.

DADONG WANG is currently a Leader of the Quantitative Imaging Research Team, Data61, CSIRO, Australia. He is also an Adjunct Professor with the University of Technology Sydney and a Conjoint Associate Professor with the University of New South Wales. His research interests include image analysis, computer vision, artificial intelligence, signal processing, and software engineering.